

# Kinematic Relations Based Nanosatellite Attitude Estimation and Rate Gyros Calibration

Demet Cilden-Guler  
Dept. of Astronautical Engineering  
Istanbul Technical University  
Istanbul, Turkey  
0000-0002-3924-5422

Chingiz Hajiyev  
Dept. of Aeronautical Engineering  
Istanbul Technical University  
Istanbul, Türkiye  
0000-0003-4115-341X

**Abstract** - In this study, the attitude angles of a nanosatellite are estimated using vector measurements from magnetometers and sun sensors. The estimation approach relies on a nontraditional filtering technique that exclusively uses a kinematic model, which is propagated by the measurements from rate gyroscopes. To address the challenge of gyro drift, bias terms are incorporated into the state vector, allowing for the estimation of these biases. The process is carried out in two distinct stages. In the first stage, singular value decomposition (SVD) is employed to determine the attitude measurements. In the second stage, an extended Kalman filter (EKF) is developed, which operates on the linear attitude measurements. These two stages are integrated into a single comprehensive algorithm, which accurately estimates both the attitude angles and gyroscope biases. To improve the accuracy of the rate gyroscope data, the gyroscope bias estimates are subtracted from the rate gyroscope measurements at each estimation step, effectively correcting the measurements. Additionally, the study highlights the effectiveness of the combined approach, where the nontraditional filtering technique provides robust performance even in the presence of noise or other errors in the system. By continuously refining the gyroscope bias estimates, the method ensures that the attitude estimation remains highly accurate over time, contributing to the overall stability and reliability of the nanosatellite's orientation system.

**Key words:** nanosatellite, attitude estimation, attitude kinematics, Kalman filter, magnetometer, sun sensor, rate gyro.

## I. INTRODUCTION

Satellite orientation can be estimated using filtering techniques that combine measurements in body coordinates and reference observations. Kalman filtering is commonly employed for satellite attitude estimation, dating back to its introduction in [1]. The rotational dynamics of satellites, however, are nonlinear, as are many other real-world systems. To address this nonlinearity, the Extended Kalman Filter (EKF) was proposed as an alternative to the standard linear Kalman filter, offering a more accurate estimate of the satellite's behavior [2]. Traditional methods for estimating satellite attitude angles and angular rates using the Kalman filter typically rely on nonlinear vector measurements due to the nonlinear nature of the mathematical models describing these measurements. In contrast, a linear measurement-based approach often uses the single-frame attitude determination method [3], which determines the attitude from vector observations at each measurement step.

In the literature, the Singular Value Decomposition (SVD) method has proven to be an efficient single-frame technique. It

is faster than the q-method and more robust than other fast methods like FOAM and ESOQ [4-6]. As the name suggests, a filter that uses the single-frame method is often referred to as a "single-frame method-aided filter." In this approach, attitude angles obtained from the SVD method are directly used as measurements within the Kalman filter. This integration results in a linear model since the state measurements come directly from SVD. The combination of SVD-based linear measurements with the EKF for attitude and rate estimation has been explored in [7-10].

To model a satellite's rotational motion in a filter, both kinematic and dynamic models can be combined. However, the dynamics model may introduce errors, such as inaccuracies in the inertia matrix [11]. For this reason, some algorithms rely solely on kinematic models, which do not introduce such uncertainties. Noisy measurements can be filtered by combining them with the corresponding models, and a kinematic model can be propagated using rate-integrating gyroscopes. However, gyro drift over time presents a challenge that can affect estimation accuracy. To mitigate this, additional terms related to gyro bias are incorporated into the state vector, allowing for estimation of these biases.

There are two primary approaches for spacecraft attitude and rate estimation: one that uses only kinematics and another that combines both kinematics and dynamics. By substituting the gyro-driven motion model with one based on the spacecraft's rotational dynamics, the need for onboard gyros can be eliminated when only kinematics is used. However, this modification requires an accurate dynamics model. To determine when to apply each strategy, the study [12] examines the critical level of uncertainty in the mass moment of inertia. In situations where uncertainties in the mass moment of inertia are expected to be less than 3%, attitude estimation using only kinematic relations may be preferable [12]. This approach allows the attitude estimation algorithm to mitigate the effects of uncertainties related to the satellite's dynamics.

In this study, a single-frame method-aided filter is presented, which operates using only the kinematics model and excludes the dynamics of the nanosatellite. Attitude angles are determined using magnetometer and sun sensor measurements, which are processed through the SVD method. These attitude angles are then used as input measurements in the proposed SVD-aided EKF filter. The structure of the paper is as follows: the next section presents the mathematical model of the satellite's rotational motion, followed by detailed explanations of the SVD and SVD-aided EKF methods. Simulations and

results are then analyzed, and the paper concludes with a summary.

## II. MATHEMATICAL MODELS

### A. Model of Attitude Kinematics

Kinematic equations can be derived using Euler's angles (yaw, pitch, and roll respectively) as,

$$\begin{bmatrix} \dot{\phi} \\ \dot{\theta} \\ \dot{\psi} \end{bmatrix} = \begin{bmatrix} 1 & s(\phi)t(\theta) & c(\phi)t(\theta) \\ 0 & c(\phi) & -s(\phi) \\ 0 & s(\phi)/c(\theta) & c(\phi)/c(\theta) \end{bmatrix} \begin{bmatrix} p \\ q \\ r \end{bmatrix}, \quad (1)$$

where  $c(\cdot)$ ,  $s(\cdot)$  and  $t(\cdot)$  are cosine, sine and tangent functions, and  $p$ ,  $q$ ,  $r$  are the components of the  $\bar{\omega}_{BR}$  vector of the body frame with respect to the reference frame.

The transformation in the angular velocities can be achieved by using the relationship between  $\bar{\omega}_{BI}$  and  $\bar{\omega}_{BR}$ ,

$$\bar{\omega}_{BR} = \bar{\omega}_{BI} - A \begin{bmatrix} 0 \\ -\omega_o \\ 0 \end{bmatrix} \quad (2)$$

where  $A$  is the transformation matrix from reference (orbit) to body coordinates,  $\omega_o$  is the orbital angular velocity.

### B. The Gyro Measurement Model

The rate gyro measurements can be modelled as,

$$\omega_{BI_m}(k) = \omega_{BI}(k) + \eta_g(k) + b_g(k) \quad (3)$$

where  $\omega_{BI} = [\omega_x \ \omega_y \ \omega_z]^T$  is the angular velocity vector of the body frame with respect to the inertial frame,  $b_g$  is the gyro bias vector and  $\eta_g$  is the zero mean white noise with normal distribution with the characteristic of,

$$E[\eta_{gk}\eta_{gj}^T] = I_{3 \times 3} \sigma_g^2 \delta_{kj}, \quad (4)$$

where  $E[\cdot]$  is the statistical averaging operator, and  $\delta_{kj}$  is the Kronecker delta function,  $\sigma_g$  is the standard deviation of rate gyro error. The characteristic of gyro biases  $b_g = [b_{g_x} \ b_{g_y} \ b_{g_z}]^T$  is given as,

$$b_g(k+1) = b_g(k) + \eta_1 \times \Delta t \quad (5)$$

where  $\eta_1$  is the zero mean white noise with normal distribution with the characteristic of

$$E[\eta_{1k}\eta_{1j}^T] = I_{3 \times 3} \sigma_{gb}^2 \delta_{kj}, \quad (6)$$

where  $\sigma_{gb}$  is the standard deviation of gyro biases.

### C. The Magnetometer Measurement Model

As the satellite navigates along its orbit, magnetic field vector differs in a relevant way with the orbital parameters. If

those parameters are known, then, magnetic field tensor vector that affects satellite can be shown as a function of time analytically. The geomagnetic field direction cosines in the orbit frame can be written in the following form:

$$B_{\alpha x}(t) = \frac{B_{\alpha x}^*(t)}{\|B_o^*\|_2}; B_{\alpha y}(t) = \frac{B_{\alpha y}^*(t)}{\|B_o^*\|_2}; B_{\alpha z}(t) = \frac{B_{\alpha z}^*(t)}{\|B_o^*\|_2} \quad (7)$$

where  $B_{\alpha x}^*(k)$ ,  $B_{\alpha y}^*(k)$  and  $B_{\alpha z}^*(k)$  are the Earth magnetic field vector components in the orbit frame,  $\|B_o^*\|_2 = \sqrt{(B_{\alpha x}^*(t))^2 + (B_{\alpha y}^*(t))^2 + (B_{\alpha z}^*(t))^2}$  is the Euclidean norm of geomagnetic field vector.

The satellite's three onboard magnetometers measure the components of the magnetic field vector in the body frame. To construct the measurement model that represents these measurements in the body frame, the measured magnetic field components must be transformed using the direction cosine matrix,  $A$ . The complete measurement model can be expressed as follows:

$$\begin{bmatrix} B_{mx}(k) \\ B_{my}(k) \\ B_{mz}(k) \end{bmatrix} = \left( A \begin{bmatrix} B_{\alpha x}(k) \\ B_{\alpha y}(k) \\ B_{\alpha z}(k) \end{bmatrix} + \eta_m(k) \right) \quad (8)$$

Here  $B_{mx}(k)$ ,  $B_{my}(k)$  and  $B_{mz}(k)$  show the measured Earth magnetic field vector components (direction cosines) in body frame as a function of time and varying Euler angles, and  $\eta_m(k)$  is the zero mean Gaussian white noise with the covariance matrix of

$$E[\eta_m(k)\eta_m^T(j)] = I_{3 \times 3} \sigma_m^2 \delta(kj) \quad (9)$$

$I_{3 \times 3}$  is the identity matrix with the dimension of  $3 \times 3$ ,  $\sigma_m$  is the standard deviation of the magnetometer error.

### D. The Sun Sensor Measurement Model

The unit sun direction vector in the Earth-Centered Inertial (ECI) frame can be computed using the linear model based on the sun's ecliptic longitude [11]. Orbital elements from the satellite's orbit propagation model are required to transform the unit sun direction vector from the ECI frame into the orbital frame. Once this transformation is completed, the model for the sun sensor measurements can be expressed as follows:

$$S_{mes} = S_b = AS_o + \eta_s, \quad (10)$$

where,  $S_o$  is the sun direction vector in the orbit frame and  $S_b$  are the sun sensor measurements in body frame which are corrupted with,  $\eta_s$ , the zero mean Gaussian white noise with the characteristic of

$$E[\eta_{sk}\eta_{sj}^T] = I_{3 \times 3} \sigma_s^2 \delta_{kj}. \quad (11)$$

where  $\sigma_s$  is the standard deviation of sun sensor measurement noise.

### III. SVD METHOD FOR ATTITUDE DETERMINATION

Attitude angles can be determined using two or more vectors by using a single-frame method minimizing Wahba's loss function in (12). We used Singular Value Decomposition (SVD) [5]. The loss is caused from the difference of the measurements from the corresponding reference models.

$$L(A) = \frac{1}{2} \sum_i a_i |b_i - Ar_i|^2 \quad (12)$$

$$B = \sum a_i b_i r_i^T \quad (13)$$

$$L(A) = \sum a_i - \text{tr}(AB^T) \quad (14)$$

where  $b_i$  is measurement vector,  $r_i$  is reference vector,  $a_i$  is non-negative weight.

$$B = USV^T = U \text{diag}([S_{11} \ S_{22} \ S_{33}])V^T \quad (15)$$

$$A_{opt} = U \text{diag}[1 \ 1 \ \det(U)\det(V)]V^T \quad (16)$$

The  $U$  and  $V$  matrices are left and right orthogonal matrices defined in SVD. They express the  $B$  matrix with primary singular values ( $S_{11}$ ,  $S_{22}$ ,  $S_{33}$ ). The Euler angle measurements can be obtained using the attitude matrix  $A_{opt}$ . Covariance matrix of the attitude angle estimation errors ( $P_{SVD}$ ) is,

$$P_{SVD} = U \text{diag}[(s_2 + s_3)^{-1} \ (s_3 + s_1)^{-1} \ (s_1 + s_2)^{-1}]U^T \quad (17)$$

where  $s_1 = S_{11}$   $s_2 = S_{22}$   $s_3 = \det(U)\det(V)S_{33}$ .

### IV. SVD-AIDED EKF FOR ATTITUDE ESTIMATION

The kinematics model of the satellite can be expressed as

$$x(k) = f[x(k-1)] + G(k, k-1)w(k-1) \quad (18)$$

$$Z(k) = Hx(k) + v(k) \quad (19)$$

where  $x(k)$  is the state vector,  $f[\cdot]$  is the nonlinear system function,  $G(k, k-1)$  is the system noise transition matrix,  $w(k-1)$  is the system noise,  $Z(k)$  is the measurement vector,  $H$  is the measurement matrix,  $v(k)$  is the measurement noise. The process and measurement noises,  $w(k)$  and  $v(k)$  are normal distributed white noises. Their expected values and covariances are,

$$\begin{aligned} E[w(k)] &= 0; E[w(k)w^T(j)] = Q(k)\delta(kj); E[v(k)] = 0; \\ E[v(k)v^T(j)] &= R(k)\delta(kj); E[w(k)v^T(j)] = 0. \end{aligned} \quad (20)$$

Rotational motion parameters can be estimated by using the following steps in the nontraditional extended Kalman filter (SVD-Aided EKF).

The covariance matrix of the extrapolation error,

$$\begin{aligned} P(k/k-1) &= \frac{\partial f[\hat{x}(k-1)]}{\partial \hat{x}(k-1)} P(k-1/k-1) \times \frac{\partial f^T[\hat{x}(k-1)]}{\partial \hat{x}(k-1)} \\ &+ G(k, k-1)Q(k-1)G^T(k, k-1) \end{aligned} \quad (21)$$

The covariance of the estimation error,

$$P(k/k) = [I - K(k)H]P(k/k-1) \quad (22)$$

Gain of the EKF,

$$K(k) = P(k/k-1)H^T [HP(k/k-1)H^T + R(k-1)]^{-1} \quad (23)$$

Innovation sequence,

$$e(k/k-1) = Z(k) - H\hat{x}(k/k-1) \quad (24)$$

Extrapolation equation,

$$\hat{x}(k/k-1) = f[\hat{x}(k-1/k-1)] \quad (25)$$

Estimate vector  $\hat{x}(k/k)$  is found as,

$$\hat{x}(k/k) = \hat{x}(k/k-1) + K(k)e(k/k-1) \quad (26)$$

where  $Q$  is the covariance matrix of the process noise.  $R$  is the covariance matrix of the measurement noise and calculated by SVD as  $R = P_{SVD}$  in each step because they both are the measurement error covariance matrices of the attitude angles. As the measurement covariance adapts itself by using the information from the SVD, the integrated filter become adaptive.

Gyroscopes, magnetometers and sun sensors are used as the attitude and rate sensors in this study. At least two vectors are measured by the star trackers and by using those vectors in the SVD sub step, attitude angle measurements are obtained.

The measurements can be presented as,

$$\begin{aligned} Z_\phi(k) &= \phi(k) + v_\phi(k) \\ Z_\theta(k) &= \theta(k) + v_\theta(k) \\ Z_\psi(k) &= \psi(k) + v_\psi(k) \end{aligned} \quad (27)$$

where  $Z_\phi(k)$ ,  $Z_\theta(k)$ ,  $Z_\psi(k)$  represent the attitude angle measurements determined by SVD method,  $v_{(\cdot)}(k)$  is the measurement noises of the attitude angles. We can call the SVD measurements as  $Z_1(k) = [Z_\phi(k) \ Z_\theta(k) \ Z_\psi(k)]^T$ . The rate gyro measurements described in (4) can be expressed as  $Z_2(k) = \omega_{Bl_m}(k)$ .  $Z(k) = Z_1(k)$  equality is used for the measurements in the filter. This means that the measurement input vector is composed of the attitude measurements from SVD. Here,  $Z_1(k)$  represents the measurements from SVD using the magnetometer and sun sensor measurements.

The corrected (bias eliminated) rate gyro measurements can be represented from the rate gyroscope measurements as

$$Z_2^{cor}(k) = Z_2(k) - \hat{b}_g(k-1) \quad (28)$$

where  $\hat{b}_g(k-1)$  is the estimated gyro bias vector by the filter. The variances of corrected angular velocity measurements can be determined as

$$\text{Cov}(Z_2^{cor}(k)) = \text{Cov}(Z_2(k)) + \text{Cov}(\hat{b}_g(k-1)) = \begin{pmatrix} \sigma_g^2 & 0 & 0 \\ 0 & \sigma_g^2 & 0 \\ 0 & 0 & \sigma_g^2 \end{pmatrix} + \begin{pmatrix} P(4,4) & 0 & 0 \\ 0 & P(5,5) & 0 \\ 0 & 0 & P(6,6) \end{pmatrix}_{k-1} \quad (29)$$

The bias-free gyroscope measurements are then fed back into the kinematic model, which is also used in the SVD-aided EKF. The augmented state vector is

$$x(k) = [\phi(k) \quad \theta(k) \quad \psi(k) \quad b_{g_x}(k) \quad b_{g_y}(k) \quad b_{g_z}(k)]^T \quad (30)$$

The structure of the whole algorithm using the kinematics model is given in Fig. 1.

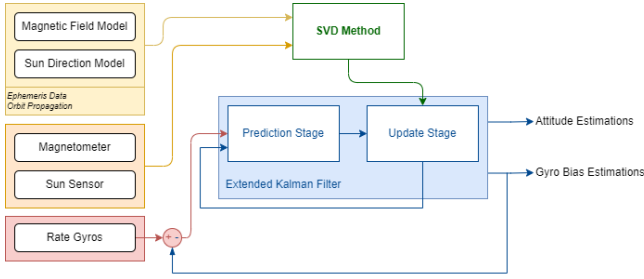


Fig.1. SVD-Aided EKF structure

As seen, the biases of the gyroscope measurements are filtered out by using the SVD-aided EKF estimations. Then, the gyroscopes measurements are fed back to the kinematics model.

## V. ANALYSIS OF SIMULATION RESULTS

In this study, we considered a nanosatellite with mass moment of inertia

$$J = \begin{bmatrix} 2.1 \times 10^{-3} & 0 & 0 \\ 0 & 2.0 \times 10^{-3} & 0 \\ 0 & 0 & 1.9 \times 10^{-3} \end{bmatrix} \text{kg.m}^2$$

having a magnetometer, sun sensors and gyroscope as attitude and rate sensors. The parameters associated with the SVD-aided EKF are presented in Table I. In this approach, the process states are estimated without incorporating the dynamics of the satellite's rotational motion in the system model. Instead, the kinematics are updated using gyro measurements that have had the bias removed, directly feeding into the estimation process without relying on the dynamics. Defined vectors in (13) are implemented as,  $b_i$  measurement vector that is obtained from the output signals of the magnetometer and sun sensor,  $r_i$  reference vector that is obtained from the Earth's magnetic field and the sun's direction vector,  $a_i$  non-negative weight which is the inverse variances of the magnetometer and sun sensor. Fig. 1

represents the estimation results of attitude angles by SVD-aided EKF method. As can be seen from the figure, the estimates are very close to the actual values. Figures 2 and 3 show the errors in estimating the gyroscope bias and the variance of the errors over time. It is concluded that SVD-aided EKF can accurately estimate the attitude angles and bias of gyroscopes using only kinematics relations.

TABLE 1. SVD-AIDED EKF PARAMETERS

Initial Covariance of the Estimation Error	$P = 0.00I_{6 \times 6}$
System Noise Transition Matrix	$G = I_{6 \times 6}$
System Noise Covariance	$Q = 0.00I_{6 \times 6}$
Measurement Matrix of System	$H = \begin{bmatrix} 1 & 0 & 0 & 0 & 0 & 0 \\ 0 & 1 & 0 & 0 & 0 & 0 \\ 0 & 0 & 1 & 0 & 0 & 0 \end{bmatrix}$

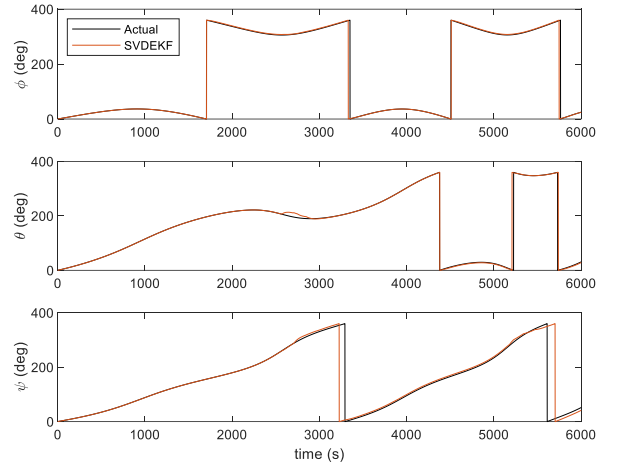


Fig.1. Attitude angles Estimation results by SVD-Aided EKF

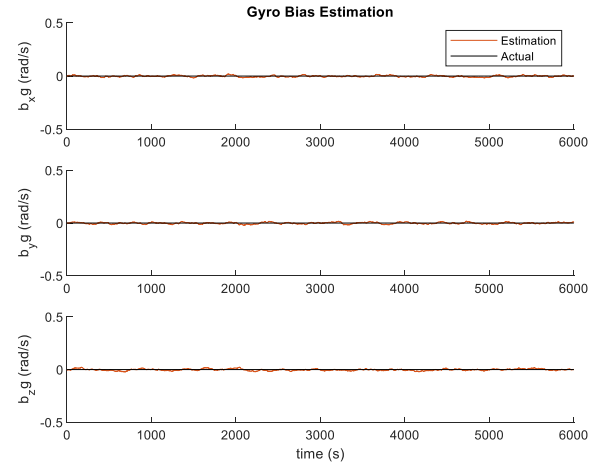


Fig.2. Gyroscope bias estimation results by SVD-Aided EKF

Corrected rate gyroscope measurements can be determined by subtracting the gyroscope bias estimates from the rate gyroscope measurements

$$Z_2^{cor}(k) = Z_2(k) - \hat{b}_g(k-1) = \omega_{Bl_m}(k) - \hat{b}_g(k-1) \quad (31)$$

A comparison of the corrected rate gyro measurements with their actual values is shown in the graphs presented in Fig. 4.

As can be seen, the corrected rate gyro measurements are very close to the actual values.

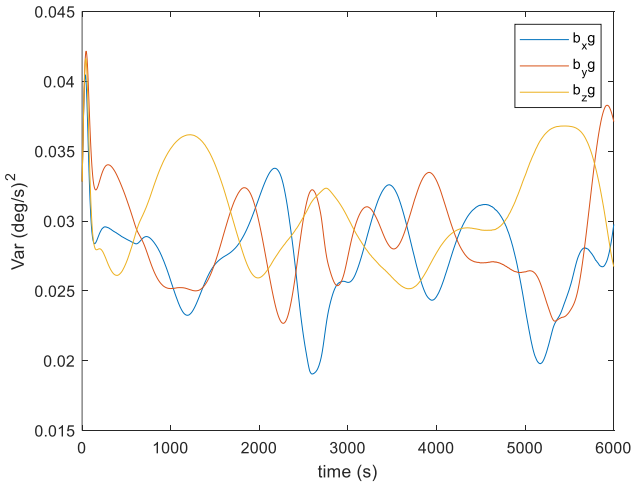


Fig.3. Variances of gyroscope bias estimation errors by SVD-Aided EKF

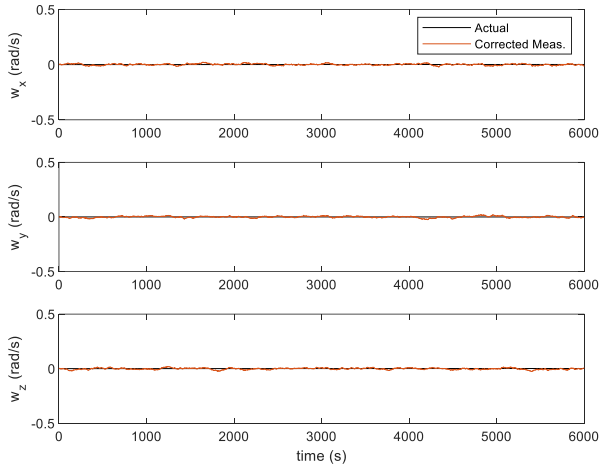


Fig.4. Corrected rate gyroscope measurements

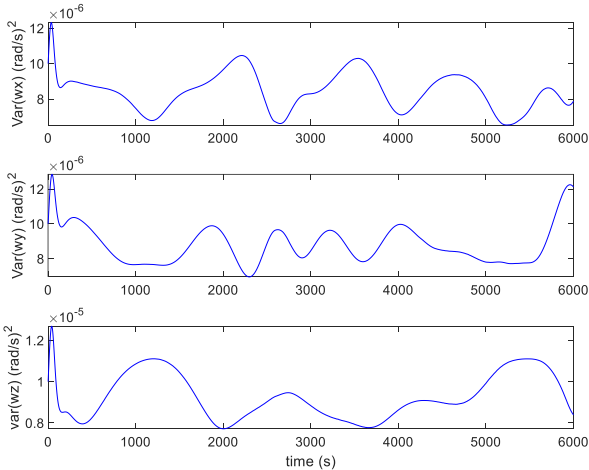


Fig.5. Variances of the corrected rate gyroscope measurements errors

The variances of the corrected rate gyroscope measurement errors, calculated using formula (31), are shown in Fig. 5. As can be seen, the variances are not constant and change depending on the accuracy of the rate gyro bias estimate.

## VI. CONCLUSIONS

This study presents a single-frame method-aided filter designed to work with only the kinematics model, excluding the dynamics of a nanosatellite. The onboard attitude and rate sensors include magnetometers, sun sensors, and gyroscopes. The magnetometer and sun sensor measurements are used to determine the attitude angles through Singular Value Decomposition (SVD), which are then fed as input measurements into the proposed filter, known as the SVD-aided EKF. This filter estimates both the attitude angles and the gyroscope biases. The estimated gyro biases are subsequently removed from the gyro measurements. After this, the bias-corrected gyro measurements are passed back into the kinematics model, which is also utilized within the SVD-aided EKF. The entire algorithm operates recursively, and the results demonstrate that the filter achieves high accuracy in estimating both attitude angles and gyro biases.

For future research, the SVD-Aided Unscented Kalman Filter (UKF) could be explored as a comparison to the SVD-Aided EKF to assess potential improvements or differences in performance.

## REFERENCES

- [1] E.J. Lefferts., F.L. Markley, M.D. Shuster, "Kalman filtering for spacecraft attitude estimation," J. Guid. Control. Dyn. 1982, vol. 5, pp. 417–429.
- [2] F.L. Markley, J.L. Crassidis, Y. Cheng, "Nonlinear attitude filtering methods, in: AIAA Guidance, Navigation, and Control Conference and Exhibit., 2005, San Francisco, California.
- [3] J.R. Wertz, "Spacecraft Attitude Determination and Control," Astrophysics and Space Science Library. D.Reidel Publishing Company, Dordrecht, Holland, 2002.
- [4] D. Cilden-Guler, E.S. Conguroglu, C. Hajiyev, "Single-frame attitude determination methods for nanosatellites," Metrol. Meas. Syst., 2017, vol. 24, pp. 313–324. doi:10.1515/mms-2017-0023
- [5] F.L. Markley, D. Mortari, "Quaternion attitude estimation using vector observations," J. Astronaut. Sci., 2000, vol. 48, pp. 359–380.
- [6] K. Vinther, K.F. Jensen, J.A. Larsen, R. Wisniewski, "Inexpensive cubesat attitude estimation using quaternions and unscented Kalman filtering," Autom. Control Aerosp., 2011, vol. 4.
- [7] C. Hajiyev, M. Bahar, "Increase of accuracy of the small satellite attitude determination using redundancy techniques," Acta Astronaut., 2002, vol. 50, pp. 673–679. doi:10.1016/s0094-5765(01)00222-3
- [8] C. Hajiyev, M. Bahar, "Attitude determination and control system design of the ITU-UUBF LEO1 satellite," Acta Astronaut., 2003, vol. 52, pp. 493–499. doi:10.1016/S0094-5765(02)00192-3
- [9] C. Hajiyev, D. Cilden, D., "Nontraditional approach to satellite attitude estimation," Int. J. Control Syst. Robot., 2016, vol. 1, pp. 19–28.
- [10] K. Mmopelwa, T.T. Ramodimo, O. Matsebe, B. Basutli, "Attitude determination and attitude estimation for earth observing 1U CubeSats: a tutorial," 2022 International Conference on Smart Applications, Communications and Networking, IEEE. DOI: 10.1109/SMARTNETS55823.2022.9994000
- [11] J.L. Crassidis, F.L. Markley, Y. Cheng, "Survey of nonlinear attitude estimation methods," J. Guid. Control. Dyn., 2007, vol. 30, pp. 12–28. doi:10.2514/1.22452
- [12] D. Cilden-Guler, C. Hajiyev, "SVD-aided EKF for nanosatellite attitude estimation based on kinematic and dynamic relations," Gyroscopy and Navigation, 2023, vol. 14, no. 4, pp. 366–379. DOI: 10.1134/S2075108724700081